

State Estimation Considering Negative Information with Switching Kalman and Ellipsoidal Filtering

Benjamin Noack*, Florian Pfaff*, Marcus Baum[†], and Uwe D. Hanebeck*

*Intelligent Sensor-Actuator-Systems Laboratory (ISAS)

Institute for Anthropomatics and Robotics

Karlsruhe Institute of Technology (KIT), Germany

benjamin.noack@ieee.org, florian.pfaff@kit.edu, uwe.hanebeck@ieee.org

[†]Institute of Computer Science

University of Göttingen, Germany

marcus.baum@cs.uni-goettingen.de

Abstract—State estimation concepts like the Kalman filter heavily rely on potentially noisy sensor data. In general, the estimation quality depends on the amount of sensor data that can be exploited. However, missing observations do not necessarily impair the estimation quality but may also convey exploitable information on the system state. This type of information—*noted as negative information*—often requires specific measurement and noise models in order to take advantage of it. In this paper, a hybrid Kalman filter concept is employed that allows using both stochastic and set-membership representations of information. In particular, the latter representation is intended to account for negative information, which can often be easily described as a bounded set in the measurement space. Depending on the type of information, the filtering step of the proposed estimator adaptively switches between Gaussian and ellipsoidal noise representations. A target tracking scenario is studied to evaluate and discuss the proposed concept.

I. INTRODUCTION

Deriving an estimate for a system’s state is a central problem in many technical applications. Dynamic state estimation methods provide the means to recursively compute an estimate based on prior knowledge about the state variables, models for the process dynamics and sensor devices, and noise characteristics. In general, these methods are designed to exploit all available sensor data. Although actual observations from sensor devices play the key role in the state estimation process, missing but expected sensor readings can also contribute to improving the estimation quality. A missing observation has to be translated into virtual measurement information before it can be exploited by the state estimation system. For this type of information, the term *negative information* has been established [1]–[4].

The concept of negative sensor information has attracted attention, in particular, in tracking and localization applications [5]. In [1], a ground moving target indicator radar constitutes the considered sensor system. Here, the state estimation system utilizes the information that missing detections can be linked to targets that do not reach the minimum detectable radial velocity. Several further radar-based tracking scenarios, where negative information can be exploited, are examined in [2] and [6]. These studies include the tracking of groups when closely spaced objects cannot be properly resolved and the tracking with phased-array radars when the beam has to be repositioned after track loss. Negative information can be

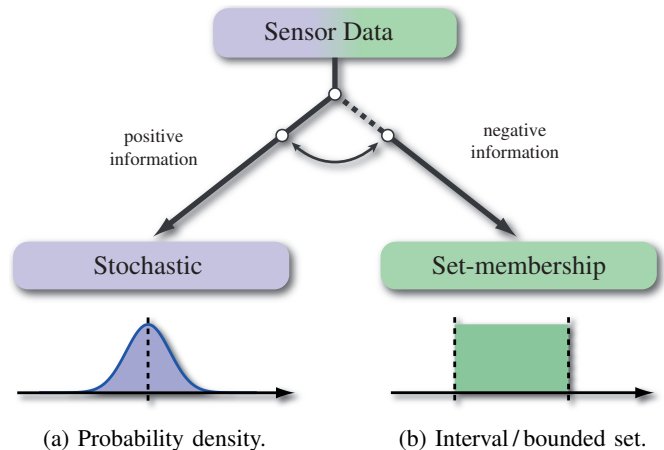


Fig. 1: Switching sensor noise model.

used to model mutual occlusions between multiple extended objects that are to be tracked [7]. For this purpose, an occlusion likelihood is constructed that assigns a probability value to each position within the sensor range and assesses how likely an object is not detected at this position. This likelihood also finds application in multiple hypothesis tracking [8]. A grid-based visibility map is considered in [9], which is employed in the probabilistic data association filter [5] to adjust the existence probability of an object.

Prior knowledge about the environment and infrastructure proves to be highly useful in defining negative information [3]. Unobserved landmarks are regarded in [4] and [10] as negative sensor evidence, which relies on prior knowledge about the probability of not observing a landmark given the robot’s pose. This approach has been further developed by [11] in order to increase robustness to detection errors when landmarks remain unobserved despite being in sensor range. While the approaches in [4], [10], and [11] are intended for localization tasks within the confined area of a RoboCup soccer field, the tracking algorithms proposed in [12] benefit from negative information in large-scale environments. The indoor positioning technique in [13] applies the concept of negative information to wireless sensor networks, where again nodes being not in range represent negative information. A similar approach is pursued in [14], where box-shaped regions of sensor coverage

are constructed for wireless sensor networks. The majority of the discussed approaches are directly concerned with tracking and localization. Within the context of simultaneous localization and mapping, but not for the localization task itself, the authors of [15] make use of negative information for the purpose of removing spurious landmarks from the map. In [16] and [17], negative information forms the foundation of event-based state estimation, where implicit measurement information is derived from the event-triggering criterion. The absence of incoming data implies that the actual sensor readings fall below some predefined threshold, which can be translated into a bounded set of possible measurement values.

The concept of negative information requires special care since the deployed estimation system cannot distinguish whether the state to be observed is out of range or the sensors fail to detect it. The design of an appropriate likelihood function for negative sensor evidence constitutes yet another problem as non-Gaussian and possibly multimodal densities have to be considered. Consequently, even linear estimation problems instantaneously turn into nonlinear ones. However, one of the most prominent methods for state estimation is the Kalman filter [18], which is optimal with respect to the mean-squared estimation error for linear models and additive white Gaussian noise. It constitutes a closed-form solution to estimation problems. In this paper, we are therefore concerned with the question of how to incorporate negative information into the Kalman filtering scheme while keeping the scheme linear and simple. As illustrated in Fig. 1, we avail ourselves a set-membership representation of negative information in place of a stochastic model. More precisely, the scheme switches between a stochastic and set-membership observation model while the former is used to account for actual sensor data and the latter represents conclusions drawn from missing sensor data. Set-membership techniques such as [19], [20] prove to be particularly well suited when measurement uncertainties can be characterized by bounded regions rather than by probability distributions. This constitutes a strong argument in favor of using bounded sets to model negative information. For instance, the area behind an obstacle or sections in a grid-based visibility map can intuitively be characterized by sets. In a similar fashion, the integration of other types of information can be realized. An important instance is human-generated data that comprises set-membership information about the state, such as a visual confirmation that an object to be tracked is localized in a bounded region.

The technique proposed in this article is based on [21] and [22], where it has been demonstrated that a combined filtering scheme can be designed that allows for a simultaneous treatment of Gaussian noise and unknown but bounded error terms represented by ellipsoids. In [17], the combined filter has been used for event-based state estimation. With this scheme, we are in the position to combine positive (stochastic) and negative (set-membership) sensor evidence with each other. Due to the switching information representation, we can further simplify the scheme and arrive at an easy-to-implement extension of the Kalman filter and its derivatives.

II. CONSIDERED PROBLEM SETUP

In the following, real-valued (random) vectors are denoted as underlined variables \underline{x} , and boldface, lowercase letters \mathbf{y} represent random errors. Matrices are written in uppercase boldface letters $\mathbf{C} \in \mathbb{R}^{n \times n}$. The matrices \mathbf{C}^{-1} and \mathbf{C}^T denote the inverse and transpose of \mathbf{C} , respectively. The vector $\hat{\underline{x}}$ is used for the mean of a random variable, an estimate of an uncertain quantity, or an observation. The matrix \mathbf{I} is the identity matrix of appropriate dimension. By $\mathcal{N}(\hat{\underline{x}}, \mathbf{C})$, the normal distribution with mean $\hat{\underline{x}}$ and covariance matrix \mathbf{C} is denoted. An ellipsoid with center $\hat{\underline{c}}$ and shape matrix \mathbf{X} is defined by $\mathcal{E}(\hat{\underline{c}}, \mathbf{X}) = \{\underline{x} \in \mathbb{R}^n \mid (\hat{\underline{c}} - \underline{x})^T \mathbf{X}^{-1} (\hat{\underline{c}} - \underline{x}) \leq 1\}$. An element of $\mathcal{E}(\hat{\underline{c}}, \mathbf{X})$ is denoted by \underline{c} .

The prediction-correction cycle of the proposed state estimation system is based on the models described in the following subsections.

A. System Model

The system dynamics are characterized by a linear discrete-time process model

$$\underline{x}_{k+1} = \mathbf{A}_k \underline{x}_k + \mathbf{B}_k \hat{\underline{u}}_k + \underline{\mathbf{w}}_k \quad (1)$$

that specifies the evolution of the state $\underline{x}_k \in \mathbb{R}^n$ from time step k to $k+1$ with system matrix $\mathbf{A}_k \in \mathbb{R}^{n \times n}$ and Gaussian noise $\underline{\mathbf{w}}_k \sim \mathcal{N}(\underline{0}, \mathbf{C}_k^{\mathbf{w}})$, $\mathbf{C}_k^{\mathbf{w}} \in \mathbb{R}^{n \times n}$. The noise process $\{\underline{\mathbf{w}}_k\}_{k \in \mathbb{N}}$ is white and independent of \underline{x}_0 . A control vector $\hat{\underline{u}}_k \in \mathbb{R}^l$ can be incorporated with control-input matrix $\mathbf{B}_k \in \mathbb{R}^{n \times l}$.

B. Observation Model

The integration of measurement information relies on two different principles, as indicated in Fig. 1. Available sensor data—denoted as *positive information*—is taken into account by employing the corresponding sensor model and noise characteristics while insights that can be gleaned from missing sensor outputs—referred to as *negative information*—are represented as unknown but bounded measurement information.

Positive Information: An observation $\hat{\underline{z}}_k \in \mathbb{R}^m$ is related to the state vector \underline{x}_k through a linear or linearized sensor model

$$\hat{\underline{z}}_k = \mathbf{H}_k \underline{x}_k + \underline{\mathbf{v}}_k, \quad (2)$$

where $\mathbf{H}_k \in \mathbb{R}^{m \times n}$ is the measurement matrix and $\underline{\mathbf{v}}_k \sim \mathcal{N}(\underline{0}, \mathbf{C}_k^{\mathbf{v}})$ is a zero-mean white Gaussian perturbation term, i.e., $\hat{\underline{z}}_k$ is a realization of \underline{z}_k , which follows a probability distribution as in Fig. 1(a).

Negative Information: With the aid of additional knowledge about the scenario, missing sensor observations can be brought into relation with exploitable information, such as areas occluded by obstacles. In this case, a missing observation implies that the state \underline{x}_k lies in the obstructed area \mathcal{O} . A more intuitive characterization of negative sensor evidence is a set of virtual observations which can be represented by the obstructed area, i.e.,

$$\hat{\underline{z}}_k^- = \mathbf{H}_k^- \underline{x}_k \in \mathcal{Z}_k^- \quad (3)$$

for $\underline{x}_k \in \mathcal{O}$. The set \mathcal{Z}_k^- can be interpreted as a blind spot of the sensor system. For example in the case of a ground

moving target indicator system [1], \mathcal{Z}_k^- can be designed as a set of virtual velocity measurements when the target is not detected, i.e., its actual radial velocity lies below the minimum detectable velocity. Other examples are discussed in Sec. VI. In the following, the set \mathcal{Z}_k^- is modeled and parameterized as an ellipsoid $\mathcal{E}(\hat{\underline{z}}_k^-, \mathbf{X}_k^v)$ with center point $\hat{\underline{z}}_k^-$ and shape matrix \mathbf{X}_k^v . As shown in Fig. 1(b), an ellipsoid becomes an interval in one dimension.

Negative information is here modeled in the measurement space but can also be translated into constraints on the state [23]. In this case, $\mathcal{E}(\hat{\underline{z}}_k^-, \mathbf{X}_k^v)$ is viewed as the ellipsoidal constraint $\mathcal{E}(\mathbf{H}_k^- \underline{x}_k, \mathbf{X}_k^v)$ in the state space [24], which may constitute a degenerate ellipsoid.

III. STATE ESTIMATION PRINCIPLES

In general, two basic directions can be isolated in state estimation theory. State estimates are computed either under the assumption of random deviations affecting the system and sensors or under the premise that errors are unknown but bounded. In particular, Kalman filtering [18] and ellipsoidal calculus [19] are the methods of choice.

A. Kalman Filtering

Given the models (1) and (2), the standard Kalman filtering scheme can be employed. Starting from an initial estimate $\hat{\underline{x}}_0^e$ with error covariance matrix \mathbf{C}_0^e , the objective is to compute an estimate $\hat{\underline{x}}_k^e$ of the state \underline{x}_k such that the covariance matrix of the random estimation error

$$\tilde{\underline{x}}_k = \hat{\underline{x}}_k^e - \underline{x}_k \quad (4)$$

is minimized with respect to the trace, which corresponds to the mean squared estimation error.

The prediction step of the Kalman filter applies the system model (1) to the current state estimate according to

$$\hat{\underline{x}}_{k+1}^p := \mathbb{E}[\underline{x}_{k+1} | \hat{\underline{z}}_{0:k}] = \mathbf{A}_k \hat{\underline{x}}_k^e + \mathbf{B}_k \hat{\underline{u}}_k \quad (5)$$

and

$$\mathbf{C}_{k+1}^p = \mathbb{E}[\tilde{\underline{x}}_{k+1} \tilde{\underline{x}}_{k+1}^T] = \mathbf{A}_k \mathbf{C}_k^e \mathbf{A}_k^T + \mathbf{C}_k^w \quad (6)$$

for the conditional mean and the error covariance matrix, respectively.

In the filtering step, the state estimate is updated with measurement information, which is related to the state by (2). By means of the Kalman gain

$$\mathbf{K}_k = \mathbf{C}_k^p \mathbf{H}_k^T (\mathbf{C}_k^v + \mathbf{H}_k \mathbf{C}_k^p \mathbf{H}_k^T)^{-1}, \quad (7)$$

the combination

$$\begin{aligned} \hat{\underline{x}}_k^e &:= \mathbb{E}[\underline{x}_k | \hat{\underline{z}}_{0:k}] = \hat{\underline{x}}_k^p + \mathbf{K}_k (\hat{\underline{z}}_k - \mathbf{H}_k \hat{\underline{x}}_k^p) \\ &= (\mathbf{I} - \mathbf{K}_k \mathbf{H}_k) \hat{\underline{x}}_k^p + \mathbf{K}_k \hat{\underline{z}}_k \end{aligned} \quad (8)$$

can be computed, which minimizes the trace of the error covariance matrix

$$\begin{aligned} \mathbf{C}_k^e &= \mathbb{E}[\tilde{\underline{x}}_k \tilde{\underline{x}}_k^T] \\ &= (\mathbf{I} - \mathbf{K}_k \mathbf{H}_k) \mathbf{C}_k^p (\mathbf{I} - \mathbf{K}_k \mathbf{H}_k)^T + \mathbf{K}_k \mathbf{C}_k^v \mathbf{K}_k^T \end{aligned} \quad (9)$$

given in the Joseph form.

The Kalman filtering scheme provides no means to directly incorporate measurement information in the form of (3). Often, coarse approximations are employed, such as a uniform distribution over the set \mathcal{Z}_k^- , which is reapproximated with a Gaussian distribution. This latter step is required to evaluate the filtering formulas (7)–(9).

B. Ellipsoidal Filtering

Set-membership state estimation techniques naturally address measurement uncertainties in the form of (3). Frequently used representations of sets are multidimensional intervals [20] or ellipsoidal sets [19], [25]. In this article, we avail ourselves of ellipsoidal bounds $\mathcal{E}(\hat{\underline{c}}, \mathbf{X})$ as they feature a parameterization that resembles Gaussian distributions, i.e., they are each parameterized by a midpoint $\hat{\underline{c}} \in \mathbb{R}^n$ and a symmetric nonnegative definite shape matrix $\mathbf{X} \in \mathbb{R}^{n \times n}$. As for normally distributed random variables, affine transformations can easily be computed by means of the corresponding transformations of the parameters, i.e.,

$$\mathbf{A} \mathcal{E}(\hat{\underline{c}}, \mathbf{X}) + \underline{b} = \mathcal{E}(\mathbf{A} \hat{\underline{c}} + \underline{b}, \mathbf{A} \mathbf{X} \mathbf{A}^T).$$

In contrast to the sum of normal random variables, the Minkowski sum of two ellipsoids, i.e., the elementwise sum, does not, in general, preserve the ellipsoidal representation, and an outer approximation

$$\mathcal{E}(\hat{\underline{c}}_1, \mathbf{X}_1) \oplus \mathcal{E}(\hat{\underline{c}}_2, \mathbf{X}_2) \subseteq \mathcal{E}(\hat{\underline{c}}_1 + \hat{\underline{c}}_2, \mathbf{X}(\omega)) \quad (10)$$

with shape matrix

$$\mathbf{X}(\omega) = \frac{1}{\omega} \mathbf{X}_1 + \frac{1}{1-\omega} \mathbf{X}_2 \quad (11)$$

has to be computed to preserve the representation. The inclusion (10) holds for every $\omega \in (0, 1)$ [19]. In general, an optimal outer approximation requires ω to be determined numerically.

In ellipsoidal state estimation, we aspire to find an ellipsoid $\mathcal{E}(\hat{\underline{x}}_k^e, \mathbf{X}_k^e)$ such that the unknown true state \underline{x}_k is included, i.e., $\underline{x}_k \in \mathcal{E}(\hat{\underline{x}}_k^e, \mathbf{X}_k^e)$. Due to the symmetry of ellipsoids, the error fulfills

$$\underline{z}_k = \hat{\underline{x}}_k^e - \underline{x}_k \in \mathcal{E}(\underline{0}, \mathbf{X}_k^e) \quad (12)$$

and also $\|\underline{z}_k\|^2 = \text{trace}(\underline{z}_k \underline{z}_k^T) \leq \text{trace}(\mathbf{X}_k^e)$. The formulas for the prediction step and the measurement update bear strong resemblance to the corresponding Kalman filter formulas. Even the intersection of ellipsoids that has to be computed to incorporate measurement information like (3) becomes a sum weighted by a gain similar to (7). The main difference between Kalman and ellipsoidal filtering lies in the computation of the uncertainty matrices. For each sum of shape matrices, a parameter ω as in (11) must be determined.

IV. COMBINED STATE ESTIMATION

Our switching observation model in Sec. II-B requires measurement updates with both standard, normally distributed observations and negative, ellipsoidally shaped observation sets. In [21], a framework for the simultaneous treatment of

stochastic and set-membership errors has been proposed. The error representations (4) and (12) coalesce into

$$\tilde{\mathbf{x}}_k + \underline{\mathbf{z}}_k = \hat{\underline{\mathbf{x}}}_k^e - \underline{\mathbf{x}}_k ,$$

which means that the estimation uncertainty is composed of a random deviation $\tilde{\mathbf{x}}_k \sim \mathcal{N}(\underline{\mathbf{0}}, \mathbf{C}_k^e)$ and an unknown but bounded term $\underline{\mathbf{z}}_k \in \mathcal{E}(\underline{\mathbf{0}}, \mathbf{X}_k^e)$. An estimate $\hat{\underline{\mathbf{x}}}_k^e$ is consequently associated with two uncertainty characteristics, i.e., an error covariance matrix \mathbf{C}_k^e and an ellipsoidal shape matrix \mathbf{X}_k^e . The mean squared error is then given by

$$\begin{aligned} \mathbb{E} [(\hat{\underline{\mathbf{x}}}_k^e - \underline{\mathbf{x}}_k)^\top (\hat{\underline{\mathbf{x}}}_k^e - \underline{\mathbf{x}}_k)] &= \mathbb{E} \left[\underbrace{(\tilde{\mathbf{x}}_k)^\top (\tilde{\mathbf{x}}_k)}_{=\text{trace}(\mathbf{C}^e)} + \underbrace{(\underline{\mathbf{z}}_k)^\top (\underline{\mathbf{z}}_k)}_{\leq \text{trace}(\mathbf{X}^e)} \right] \\ &\leq \text{trace}(\mathbf{C}_k^e + \mathbf{X}_k^e) . \end{aligned} \quad (13)$$

In the prediction step of the combined filter, mean and covariance matrix are still given by (5) and (6). In addition, the predicted shape matrix has to be computed by

$$\mathbf{X}_{k+1}^p(\omega) = \frac{1}{\omega} \mathbf{A}_k \mathbf{X}_k^e \mathbf{A}_k^\top + \frac{1}{1-\omega} \mathbf{X}_k^w \quad (14)$$

with $\omega \in (0, 1)$, where $\mathcal{E}(\underline{\mathbf{0}}, \mathbf{X}_k^w)$ accounts for unknown but bounded errors affecting the system. In the prediction step, the parameter ω can be determined in closed form for the purpose of minimizing the bound (13).

In the filtering step, the gain has to incorporate both stochastic and set-membership measurement uncertainties and is given by

$$\begin{aligned} \mathbf{K}_k(\omega) &= \left(\frac{1}{\omega} \mathbf{X}_k^p \mathbf{H}_k^\top + \mathbf{C}_k^p \mathbf{H}_k^\top \right) \cdot \\ &\left(\frac{1}{\omega} \mathbf{H}_k \mathbf{X}_k^p \mathbf{H}_k^\top + \frac{1}{1-\omega} \mathbf{X}_k^v + \mathbf{H}_k \mathbf{C}_k^p \mathbf{H}_k^\top + \mathbf{C}_k^v \right)^{-1} , \end{aligned} \quad (15)$$

where \mathbf{X}_k^v is the shape matrix of the bounding ellipsoid for the set-membership component of the measurement uncertainty. Evidently, the gain also depends on the weighting parameter from (11). In line with (8) and (9), estimate and covariance matrix are updated according to

$$\hat{\underline{\mathbf{x}}}_k^e(\omega) = (\mathbf{I} - \mathbf{K}_k(\omega) \mathbf{H}_k) \hat{\underline{\mathbf{x}}}_k^p + \mathbf{K}_k(\omega) \hat{\underline{\mathbf{z}}}_k \quad (16)$$

and

$$\begin{aligned} \mathbf{C}_k^e(\omega) &= (\mathbf{I} - \mathbf{K}_k(\omega) \mathbf{H}_k) \mathbf{C}_k^p (\mathbf{I} - \mathbf{K}_k(\omega) \mathbf{H}_k)^\top \\ &+ \mathbf{K}_k(\omega) \mathbf{C}_k^v \mathbf{K}_k(\omega)^\top , \end{aligned} \quad (17)$$

respectively. The updated shape matrix for the set-membership uncertainty becomes

$$\begin{aligned} \mathbf{X}_k^e(\omega) &= \frac{1}{\omega} (\mathbf{I} - \mathbf{K}_k(\omega) \mathbf{H}_k) \mathbf{X}_k^p (\mathbf{I} - \mathbf{K}_k(\omega) \mathbf{H}_k)^\top \\ &+ \frac{1}{1-\omega} \mathbf{K}_k(\omega) \mathbf{X}_k^v \mathbf{K}_k(\omega)^\top , \end{aligned} \quad (18)$$

which is of the form (11). Each $\omega \in (0, 1)$ is admissible, but the parameter is typically determined to minimize $\text{trace}(\mathbf{C}_k^e(\omega) + \mathbf{X}_k^e(\omega))$, which is the upper bound in (13). A one-dimensional search in $[0, 1]$ gives the solution to the convex optimization problem [19] for determining the trace-minimal ω .

The combined filtering scheme has been designed for process and sensor models that are simultaneously affected by random and unknown but bounded noise terms. For the treatment of negative information, we do not need to exploit the full potential of the combined estimation method and can simplify the above formulas, as discussed in the subsequent section.

V. FILTERING WITH SWITCHING GAINS

The combined filter [21] has been designed to deal with noise terms that consist of both a random and a set-bounded component. In the considered setup, either a measurement is available and is characterized by a standard probabilistic model or negative information is to be exploited. Hence, the sensor model is either purely stochastic or purely set-membership, and the filtering scheme can be simplified and summarized as follows.

A. Initialization

The initialization of the proposed filter is essentially the same as for the standard Kalman filter. Besides the prior mean $\hat{\underline{\mathbf{x}}}_0$ and covariance matrix \mathbf{C}_0 , the shape matrix can be initialized with $\mathbf{X}_0 = \mathbf{0}$ as it is assumed that set-membership information is only introduced when negative information comes into play.

B. Prediction Step

The first simplification is obtained in the prediction step. The formulas (5) and (6) are applied to the current estimate $\hat{\underline{\mathbf{x}}}_k^e$ and \mathbf{C}_k^e , respectively, while formula (14) for the shape matrix reduces to

$$\mathbf{X}_{k+1}^p = \mathbf{A}_k \mathbf{X}_k^e \mathbf{A}_k^\top \quad (19)$$

since no unknown but bounded error terms are assumed to affect the system dynamics (1). Hence, the prediction step is independent of the parameter ω .

C. Measurement Update

The update step of the proposed filter depends on whether positive or negative information is to be incorporated. In particular, the sensor models in Sec. II-B lead to different gains.

Positive Information: The update formulas (16)-(18) can be significantly simplified if actual sensor data according to (2) are available, i.e., set-membership uncertainty is assumed to be $\mathbf{X}_k^v = \mathbf{0}$. The gain (15) becomes

$$\begin{aligned} \mathbf{K}_k^+ &= (\mathbf{X}_k^p \mathbf{H}_k^\top + \mathbf{C}_k^p \mathbf{H}_k^\top) \cdot \\ &(\mathbf{H}_k \mathbf{X}_k^p \mathbf{H}_k^\top + \mathbf{H}_k \mathbf{C}_k^p \mathbf{H}_k^\top + \mathbf{C}_k^v)^{-1} , \end{aligned}$$

which is now independent of the parameter ω . In particular, it reduces to the Kalman gain (7) in case of $\mathbf{X}_k^p = \mathbf{0}$. The gain has to be applied in (16) and (17) in order to obtain the updated estimate

$$\hat{\underline{\mathbf{x}}}_k^e = (\mathbf{I} - \mathbf{K}_k^+ \mathbf{H}_k) \hat{\underline{\mathbf{x}}}_k^p + \mathbf{K}_k^+ \hat{\underline{\mathbf{z}}}_k$$

and the corresponding updated covariance matrix

$$\mathbf{C}_k^e = (\mathbf{I} - \mathbf{K}_k^+ \mathbf{H}_k) \mathbf{C}_k^p (\mathbf{I} - \mathbf{K}_k^+ \mathbf{H}_k)^T + \mathbf{K}_k^+ \mathbf{C}_k^y (\mathbf{K}_k^+)^T.$$

The shape matrix (18) is updated according to the simple formula

$$\mathbf{X}_k^e = (\mathbf{I} - \mathbf{K}_k^+ \mathbf{H}_k) \mathbf{X}_k^p (\mathbf{I} - \mathbf{K}_k^+ \mathbf{H}_k)^T. \quad (20)$$

Apparently, this measurement update does not require a minimization over the parameter ω .

Negative Information: Negative sensor evidence is modeled as an ellipsoidal set of expected observations (3), which can be expressed as an unknown but bounded measurement error

$$\hat{\underline{z}}_k^- - \mathbf{H}_k^- \underline{x}_k = \underline{v}_k \in \mathcal{E}(\underline{0}, \mathbf{X}_k^y) \quad (21)$$

around the virtual observation $\hat{\underline{z}}_k^-$. With $\mathbf{C}_k^y = \mathbf{0}$, the required gain yields

$$\mathbf{K}_k^-(\omega) = \left(\frac{1}{\omega} \mathbf{X}_k^p (\mathbf{H}_k^-)^T + \mathbf{C}_k^p (\mathbf{H}_k^-)^T \right) \cdot \left(\frac{1}{\omega} \mathbf{H}_k^- \mathbf{X}_k^p (\mathbf{H}_k^-)^T + \frac{1}{1-\omega} \mathbf{X}_k^z + \mathbf{H}_k^- \mathbf{C}_k^p (\mathbf{H}_k^-)^T \right)^{-1}$$

and is used in (16) and (18) to compute the updated mean

$$\hat{\underline{x}}_k^e(\omega) = (\mathbf{I} - \mathbf{K}_k^-(\omega) \mathbf{H}_k) \hat{\underline{x}}_k^p + \mathbf{K}_k^-(\omega) \hat{\underline{z}}_k^-$$

and shape matrix

$$\mathbf{X}_k^e(\omega) = \frac{1}{\omega} (\mathbf{I} - \mathbf{K}_k^-(\omega) \mathbf{H}_k) \mathbf{X}_k^p (\mathbf{I} - \mathbf{K}_k^-(\omega) \mathbf{H}_k)^T + \frac{1}{1-\omega} \mathbf{K}_k^-(\omega) \mathbf{X}_k^y \mathbf{K}_k^-(\omega)^T,$$

respectively. Due to the absence of a stochastic perturbation term, the covariance matrix becomes

$$\mathbf{C}_k^e(\omega) = (\mathbf{I} - \mathbf{K}_k^-(\omega) \mathbf{H}_k) \mathbf{C}_k^p (\mathbf{I} - \mathbf{K}_k^-(\omega) \mathbf{H}_k)^T.$$

As stated in Sec. IV, ω can be chosen from the interval (0, 1). The optimal choice of ω minimizes $\text{trace}(\mathbf{C}_k^e(\omega) + \mathbf{X}_k^e(\omega))$, which is a bound on the mean squared estimation error.

With this switching filtering scheme, a numerical determination of the trace-minimizing parameter ω is only necessary when negative information is to be exploited. Then, measurement information is purely modeled as a set. In the prediction step and the update with positive information, the method essentially reduces to the standard Kalman filter with the additional computation of (19) and (20). In each processing step, all three parameters, the estimate, error covariance, and shape matrix, are updated. The trace of the sum of covariance and shape matrix provides a bound on the maximum possible mean squared error in each processing step.

The proposed method constitutes an easy-to-implement solution for integrating the concept of negative information into the Kalman filtering scheme and its derivatives such as the extended Kalman filter. As a major advantage, set-membership information is directly incorporating and does not need to be approximated by a Gaussian or uniform distribution, which leads to additional errors or to nonlinear estimation problems.

VI. EXAMPLE AND DISCUSSION

In order to illustrate the proposed concept, a simulated tracking scenario is studied where three examples of negative information are given. In Fig. 2, the green solid line represents the true trajectory that is to be estimated and is based on the discrete-time motion model of a differential drive robot. The process and observation models used in the tracking system are described in Subsec. VI-A and Subsec. VI-B, respectively. The results are discussed in Subsec. VI-C.

A. System Model

The actual motion model is unknown to the tracking system. Instead, a near-constant-acceleration model [26] is used in the prediction step of the Kalman filter in order to characterize the process dynamics. For this purpose, the state is modeled as a six-dimensional vector that consists of position, velocity, and acceleration in each of the two Cartesian coordinates x_1 and x_2 . The model is accordingly given by

$$\underline{x}_{k+1} = \begin{bmatrix} \mathbf{A}_{x_1} & \mathbf{0} \\ \mathbf{0} & \mathbf{A}_{x_2} \end{bmatrix} \underline{x}_k + \underline{w}_k, \quad \underline{w}_k \sim \mathcal{N}\left(\underline{0}, \begin{bmatrix} \mathbf{C}_{x_1}^w & \mathbf{0} \\ \mathbf{0} & \mathbf{C}_{x_2}^w \end{bmatrix}\right).$$

For each coordinate, the system and covariance matrices are

$$\mathbf{A}_{x_1} = \mathbf{A}_{x_2} = \begin{bmatrix} 1 & \delta & \delta^2/2 \\ 0 & 1 & \delta \\ 0 & 0 & 1 \end{bmatrix}, \quad \mathbf{C}_{x_1}^w = \mathbf{C}_{x_2}^w = \begin{bmatrix} \delta^5/20 & \delta^4/8 & \delta^3/6 \\ \delta^4/8 & \delta^3/3 & \delta^2/2 \\ \delta^3/6 & \delta^2/2 & \delta \end{bmatrix}$$

with $\delta = 0.7$. Note that components $(\underline{x}_k)_1$ and $(\underline{x}_k)_4$ of the state relate to the position.

B. Observation Models

Positive Information: Two physical sensors are simulated. A GNSS-like system directly measures the position and is corrupted by Gaussian noise $\underline{v}_{\text{GNSS}} \sim \mathcal{N}(\begin{bmatrix} 0 \\ 0 \end{bmatrix}, \begin{bmatrix} 4 & 0 \\ 0 & 4 \end{bmatrix})$. The measurement matrix is the identity with respect to the position vector, and the model is

$$\hat{\underline{z}}_{\text{GNSS}} = \begin{bmatrix} 1 & 0 & 0 & 0 & 0 & 0 \\ 0 & 0 & 0 & 1 & 0 & 0 \end{bmatrix} \underline{x} + \underline{v}_{\text{GNSS}}.$$

This sensor is available at all time steps except for the tunnel.

The second sensor at position l provides range measurements

$$z_{\text{dist}} = \|\hat{\underline{x}} - \underline{l}\|_2 + \underline{v}_{\text{dist}}$$

with noise characteristics $\underline{v}_{\text{dist}} \sim \mathcal{N}(0, 0.5)$. The measurement matrix is obtained by linearization as it is done in the extended Kalman filter and yields

$$\mathbf{H}_{\text{dist}} = \frac{1}{\|\hat{\underline{x}}_k^p - \underline{l}\|} \begin{bmatrix} (\hat{\underline{x}}_k^p)_{1-L_1} & 0 & 0 & 0 & 0 & 0 \\ 0 & 0 & 0 & (\hat{\underline{x}}_k^p)_{4-L_2} & 0 & 0 \end{bmatrix}, \quad (22)$$

where the current estimate $\hat{\underline{x}}_k^p$ serves as operating point for the Taylor series expansion. Range measurements are not available inside the tunnel and behind the obstacle, which is indicated by gray areas in Fig. 2.

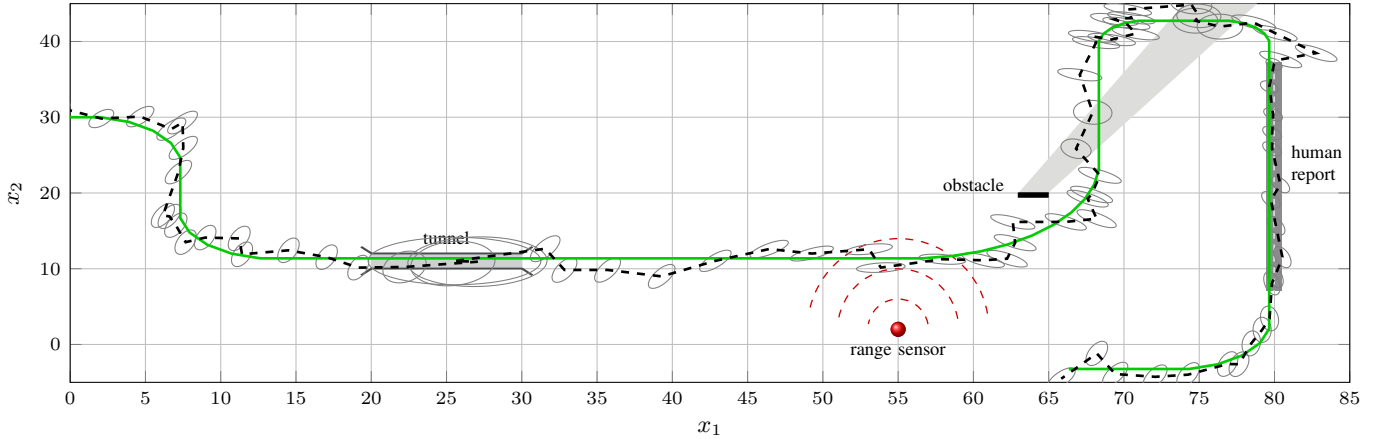
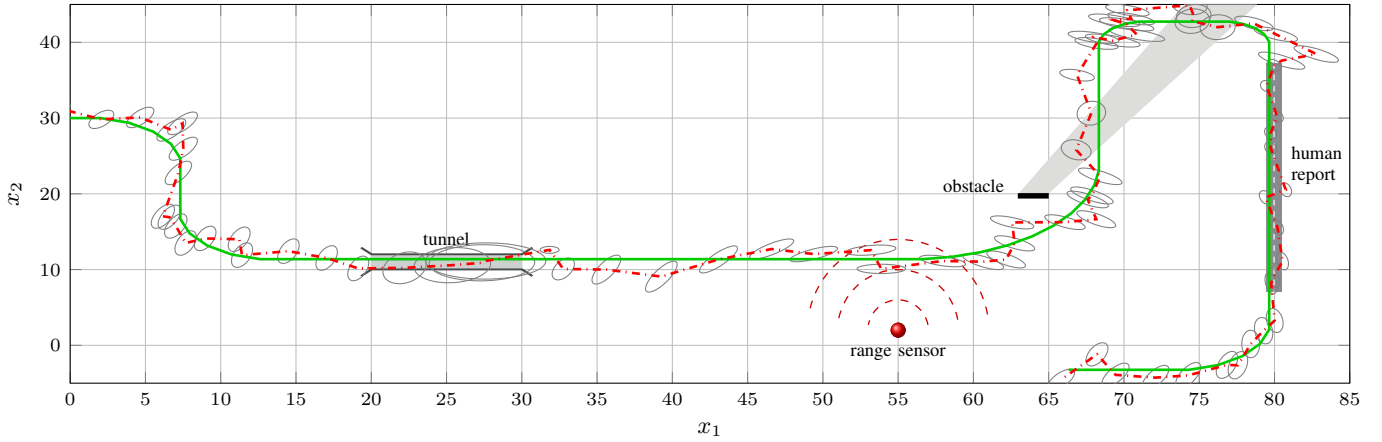
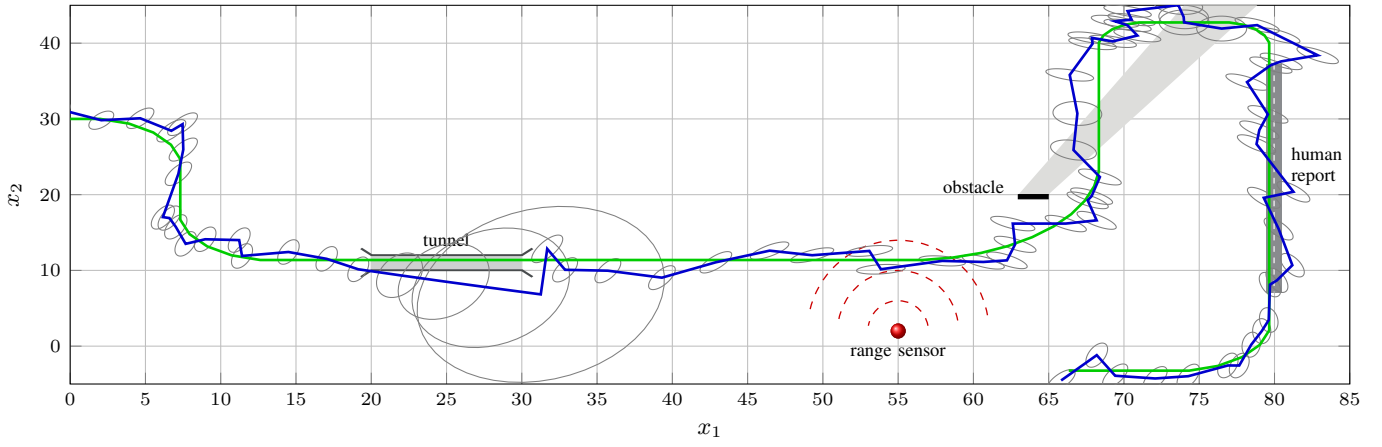


Fig. 2: Tracking results without (\rightarrow), with naive (\dashrightarrow), and with proposed (\dashrightarrow) model of negative information compared with ground truth (\rightarrow).

Negative Information: The tracking system can exploit knowledge about the obstructed areas. In the proposed concept, it is assumed that the object is detected when being in range of the sensors. Hence, missing observations are solely caused by the obstacles. In order to take into account detection errors the algorithm has to be extended to incorporate a model of detection probabilities, which is subject of future work.

In order to represent the tunnel as negative sensor evidence, the entire area of the tunnel is circumscribed by an ellipsoid. An ellipsoidal bound for the rectangular tunnel of length 5 and width $\sqrt{2}$ can easily be computed: The tunnel can be written as the Minkowski sum (10) of the degenerate ellipsoids $\mathcal{E}(\begin{bmatrix} 25 \\ 0 \end{bmatrix}, \begin{bmatrix} 25 & 0 \\ 0 & 0 \end{bmatrix})$ and $\mathcal{E}(\begin{bmatrix} 0 \\ 11 \end{bmatrix}, \begin{bmatrix} 0 & 0 \\ 0 & 2 \end{bmatrix})$. The error shape matrix $\mathbf{X}_{\text{tunnel}}^v$ of the bounding ellipsoid can then be computed

by (11). The center of the tunnel serves as the negative observation $\hat{z}_{\text{tunnel}}^- = \begin{bmatrix} 25 \\ 11 \end{bmatrix}$, and the virtual measurement equation (21) becomes

$$\hat{z}_{\text{tunnel}}^- - \begin{bmatrix} 1 & 0 & 0 & 0 & 0 & 0 \\ 0 & 0 & 0 & 1 & 0 & 0 \end{bmatrix} \underline{x}_k = \underline{v}_{\text{tunnel}} \in \mathcal{E}(0, \mathbf{X}_{\text{tunnel}}^v). \quad (23)$$

Missing range measurements can be traced back to the tunnel or the obstacle. While the first case is covered by (23), the obstructed area for the second case is more difficult to model due to the nonlinear sensor model.

As illustrated in Fig. 3, a simple solution consists of projecting the obstacle onto the x_1 -axis at the estimated x_2 -position of the robot, such that the projected length of the obstacle may then serve as a bound on the robot's x_1 -position. The projected obstacle is an interval, i.e., an one-dimensional ellipsoid $\mathcal{E}(\hat{z}_{\text{obst}}^-, (d_{\text{obst}}/2)^2)$, where d_{obst} is the diameter¹ of the interval. The observation model hence yields

$$\hat{z}_{\text{obst}}^- - [1, 0, 0, 0, 0, 0] \underline{x}_k = \underline{v}_{\text{obst}} \in \mathcal{E}(0, (d_{\text{obst}}/2)^2). \quad (24)$$

Such an approach is similar to the linearization in (22), where the model also depends on the current estimate, and is susceptible to approximation errors.

As a third example of negative sensor evidence, human-generated data is simulated which represents a visual confirmation that the vehicle is on a road. This confirmation can rather be viewed as positive evidence but is too imprecise to be represented by an explicit measurement model (2). The width of the road is considered to be a set-membership measurement of the robot's x_1 -position, and the corresponding model is

$$\hat{z}_{\text{street}}^- - [1, 0, 0, 0, 0, 0] \underline{x}_k = \underline{v}_{\text{street}} \in \mathcal{E}(0, 0.25), \quad (25)$$

where $\hat{z}_{\text{street}}^- = 80$ is the center of the street. This model is similar to (24). However, in (24), the parameters \hat{z}_{obst}^- and d_{obst} are approximations that depend on the current estimate.

C. Evaluation

Fig. 2(a) depicts the estimated trajectory that is computed by means of an extended Kalman filter. Additional information has not been incorporated and in particular, the track is lost inside the tunnel. Furthermore, the covariance ellipses of each position estimate are drawn. In contrast, the improved estimates in Fig. 2(b) and Fig. 2(c) have been obtained by exploiting negative information. Fig. 2(b) shows the results of a naive approach, where the ellipsoids in (23)-(25) are replaced by Gaussian noise. The covariance matrices correspond to the shape matrices of the ellipsoids. The results of the proposed filter are depicted in Fig. 2(c), where the drawn ellipses represent the combined uncertainty $\mathbf{C}_k^e + \mathbf{X}_k^e$. Significant improvements can be achieved for the tunnel and the street. The first time the vehicles passes the area occluded by the obstacle, an improvement could be achieved; the second time,

¹An interval of length d with center point c can be represented as the one-dimensional ellipsoid $\mathcal{E}(c, (d/2)^2)$.

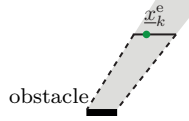
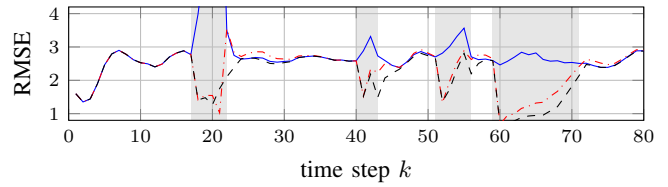
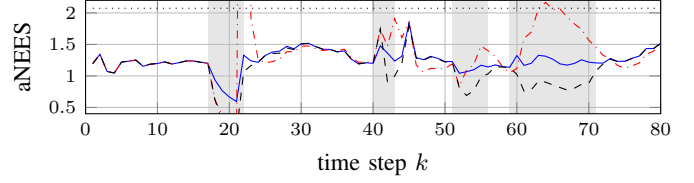


Fig. 3: Projection.



(a) RMSE for the tracking systems used in Fig. 2.



(b) Average weighted MSE for the tracking systems used in Fig. 2.

Fig. 5: Analysis of error after 2000 Monte Carlo runs. Shaded areas relate to sections where negative information can be exploited.

the vehicle moves almost tangential to the sensor and the improvement is marginal.

An important observation is that the uncertainty ellipses in Fig. 2(b) and Fig. 2(c) still exceed the area of the tunnel or street due to the stochastic prediction and sensor models. In the tunnel, negative evidence is the only exploitable information, and the uncertainty ellipse therefore converges to the bounding ellipse $\mathcal{E}(\hat{z}_{\text{tunnel}}^-, \mathbf{X}_{\text{tunnel}}^v)$, which represents a coarse approximation of the tunnel.

For comparison, Fig. 4 shows estimation results with a different model for the tunnel. Here, the

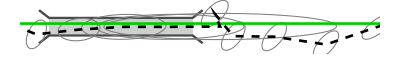


Fig. 4: Different model for tunnel.

tunnel is modeled in the same fashion as the street; only its width is used as a bound on component x_2 of the state vector. In this case, the uncertainty ellipse adapts to the x_2 -boundaries but grows unbounded in the x_1 -direction as long as the vehicle is inside the tunnel. In Fig. 2(a), where no additional information has been exploited, the covariance ellipse grows unbounded even in every direction.

In Fig. 2, the naive and the proposed approach display a similar performance; the covariance ellipses related to the naive approach even appear to be smaller than the combined uncertainty ellipses. However, as depicted in Fig. 5(a), the root mean squared error (RMSE) after 2000 Monte Carlo runs reveals that the proposed approach shows a better performance. The naive approach yields smaller covariance ellipses because the actual estimation error is underestimated, i.e., it is too optimistic. This can be seen from the RMSE, which exceeds the RMSE of the standard Kalman filter after the tunnel and street sections. This problem becomes more apparent when Fig. 5(b) is studied. The average normalized estimation error squared (NEES) [27] reveals that the naive approach reports very optimistic results compared to the Kalman filter, which does not exploit negative information and is rather conservative. The reason for this behavior is that the naive approach may provide overconfident results due to the coarse model of negative information, and the NEES even exceeds

the lower 95% probability region (dotted line). By contrast, the proposed approach displays an improved performance and reports rather conservative results. Finally, it is important to emphasize that a set-membership uncertainty representation constitutes a systematic, though simple, approach for modeling negative information, whereas it can be difficult to find an appropriate probabilistic representation for negative information. Non-Gaussian likelihoods appear to be a good option to model negative information but then require more involved filtering techniques. A comparison to such a nonlinear approach is subject of future work.

VII. CONCLUSION

The benefits that can be drawn from negative information stand in contrast to difficulties related to the representation and construction of the corresponding likelihood functions. Instead of using such a possibly non-Gaussian density, a set-membership representation of negative information has been utilized in this work. In particular, the treatment of ellipsoidal sets can easily be integrated in a generalized Kalman filtering scheme as the corresponding shape matrices have a strong analogy to covariance matrices. The proposed filter switches between two representations of measurement uncertainty. Available sensor data is incorporated according to a stochastic sensor model while evidence from missing observations is associated with a set-membership measurement model. As a result, each estimate is provided with both a stochastic and a set-membership uncertainty description. The measurement update with negative information involves the computation of a scalar weighting parameter. Consequently, the problem of incorporating negative information has been boiled down to the simple problem of determining this parameter. The good performance of the proposed filtering scheme reflects the fact that set-membership representations are well-suited to model negative sensor information.

ACKNOWLEDGMENT

This work was supported by the German Research Foundation (DFG) under grant NO 1133/1-1.

REFERENCES

- [1] C. S. Agate, R. M. Wilkerson, and K. J. Sullivan, "Utilizing Negative Information to Track Ground Vehicles through Move-Stop-Move Cycles," in *Proceedings of SPIE – Signal Processing, Sensor Fusion, and Target Recognition XIII*, vol. 5429, Orlando, Florida, USA, Apr. 2004.
- [2] W. Koch, "On 'Negative' Information in Tracking and Sensor Data Fusion: Discussion of Selected Examples," in *Proceedings of the 7th International Conference on Information Fusion (Fusion 2004)*, Stockholm, Sweden, Jun. 2004.
- [3] S. Thrun, W. Burgard, and D. Fox, *Probabilistic Robotics*, ser. Intelligent Robotics and Autonomous Agents. MIT Press, 2005.
- [4] J. Hoffmann, M. Spranger, D. Göhring, and M. Jüngel, "Making Use Of What You Don't See: Negative Information In Markov Localization," in *Proceedings of the 2005 IEEE/RSJ International Conference on Intelligent Robots and Systems (IROS 2005)*, Edmonton, Canada, Aug. 2005.
- [5] Y. Bar-Shalom and W. D. Blair, Eds., *Multitarget/Multisensor Tracking: Applications and Advances – Volume III*. Artech House, 2000.
- [6] W. Koch, "On Exploiting 'Negative' Sensor Evidence for Target Tracking and Sensor Data Fusion," *Information Fusion*, vol. 8, no. 1, pp. 28–39, Jan. 2005.

- [7] K. Wyffels and M. Campbell, "Modeling and Fusing Negative Information For Dynamic Extended Multi-object Tracking," in *Proceedings of the 2013 IEEE International Conference on Robotics and Automation (ICRA 2013)*, Karlsruhe, Germany, May 2013.
- [8] K. Wyffels and M. Campbell, "Negative Observations for Multiple Hypothesis Tracking of Dynamic Extended Objects," in *Proceedings of the 2014 American Control Conference (ACC 2014)*, Portland, Oregon, USA, Jun. 2014.
- [9] K. Tischler and H. S. Vogt, "A Sensor Data Fusion Approach for the Integration of Negative Information," in *Proceedings of the 10th International Conference on Information Fusion (Fusion 2007)*, Quebec, Canada, Jul. 2007.
- [10] J. Hoffmann, M. Spranger, D. Göhring, and M. Jüngel, "Further Studies on the Use of Negative Information in Mobile Robot Localization," in *Proceedings of the 2006 IEEE International Conference on Robotics and Automation (ICRA 2006)*, Orlando, Florida, USA, May 2006.
- [11] T. Hester and P. Stone, "Negative Information and Line Observations for Monte Carlo Localization," in *Proceedings of the 2008 IEEE International Conference on Robotics and Automation (ICRA 2008)*, Pasadena, California, USA, May 2008.
- [12] M. Shan, S. Worrall, and E. Nebot, "Probabilistic Long-term Vehicle Motion Prediction and Tracking in Large Environments," *IEEE Transactions on Transportation Systems*, vol. 14, no. 2, pp. 539–552, Jun. 2013.
- [13] M. Albano, S. Hadzic, and J. Rodriguez, "Use of Negative Information in Positioning and Tracking Algorithms," *Telecommunication Systems*, vol. 53, no. 3, pp. 285–298, Jul. 2013.
- [14] A. Baggio and K. Langendoen, "Monte Carlo Localization for Mobile Wireless Sensor Networks," *Ad Hoc Networks*, vol. 6, no. 5, pp. 718–733, Jul. 2008.
- [15] M. Montemerlo and S. Thrun, "Simultaneous Localization and Mapping with Unknown Data Association Using FastSLAM," in *Proceedings of the 2003 IEEE International Conference on Robotics and Automation (ICRA 2003)*, Taipei, Taiwan, Sep. 2003.
- [16] J. Sijs, B. Noack, M. Lazar, and U. D. Hanebeck, *Event-Based Control and Signal Processing*. CRC Press, Nov. 2015, ch. Time-Periodic State Estimation with Event-Based Measurement Updates, pp. 261–279.
- [17] J. Sijs, B. Noack, and U. D. Hanebeck, "Event-based State Estimation with Negative Information," in *Proceedings of the 16th International Conference on Information Fusion (Fusion 2013)*, Istanbul, Turkey, Jul. 2013.
- [18] R. E. Kalman, "A New Approach to Linear Filtering and Prediction Problems," *Transactions of the ASME - Journal of Basic Engineering*, vol. 82, pp. 35–45, 1960.
- [19] A. B. Kurzhanski and I. Vályi, *Ellipsoidal Calculus for Estimation and Control*. Birkhäuser, 1997.
- [20] L. Jaulin, M. Kieffer, O. Didrit, and É. Walter, *Applied Interval Analysis: With Examples in Parameter and State Estimation, Robust Control and Robotics*. London: Springer, 2001.
- [21] B. Noack, F. Pfaff, and U. D. Hanebeck, "Optimal Kalman Gains for Combined Stochastic and Set-Membership State Estimation," in *Proceedings of the 51st IEEE Conference on Decision and Control (CDC 2012)*, Maui, Hawaii, USA, Dec. 2012.
- [22] B. Noack, *State Estimation for Distributed Systems with Stochastic and Set-membership Uncertainties*, ser. Karlsruhe Series on Intelligent Sensor-Actuator-Systems 14. Karlsruhe, Germany: KIT Scientific Publishing, 2013.
- [23] D. Simon, "Kalman Filtering with State Constraints: A Survey of Linear and Nonlinear Algorithms," *IET Control Theory & Applications*, vol. 4, no. 8, pp. 1303–1318, Aug. 2010.
- [24] B. Noack, M. Baum, and U. D. Hanebeck, "State Estimation for Ellipsoidally Constrained Dynamic Systems with Set-membership Pseudo Measurements," in *Proceedings of the 2015 IEEE International Conference on Multisensor Fusion and Integration for Intelligent Systems (MFI 2015)*, San Diego, California, USA, Sep. 2015.
- [25] F. L. Chernousko, *State Estimation for Dynamic Systems*. CRC Press, 1994.
- [26] X.-R. Li and V. P. Jilkov, "Survey of Maneuvering Target Tracking III. Measurement Models," in *Proceedings of SPIE – Signal and Data Processing of Small Targets 2001*, San Diego, California, USA, Jul. 2001.
- [27] Y. Bar-Shalom, X.-R. Li, and T. Kirubarajan, *Estimation with Applications to Tracking and Navigation: Theory, Algorithms, and Software*. John Wiley & Sons, 2001.